Synchronization of sensory gamma oscillations promotes multisensory communication

Abbreviated: Cross-modal gamma coupling

Jonas Misselhorn[1], Bettina C. Schwab[1], Till R. Schneider[1], Andreas K. Engel[1]

[1] Department of Neurophysiology and Pathophysiology, University Medical Center Hamburg-Eppendorf, 20246 Hamburg, Germany

Corresponding author: j.misselhorn@uke.de, phone: +49 (0) 40 7410 - 55132

Conflict of interest

The authors declare no competing financial interests.

Acknowledgements

This work was supported by grants from the DFG (SFB 936/A3/Z1 and SFB TRR 169/B1 to AKE; SPP 1665/SCHN 1511/1-2 to TRS) and the EU (ERC-2010-AdG-269716 to AKE). The authors would like to thank Karin Deazle for help with recruitment of participants and data recording.

Abstract

Rhythmic neuronal activity in the gamma range is a signature of active cortical processing and its synchronization across distant sites has been proposed as a fundamental mechanism of network communication. While this has been shown within sensory modalities, we tested whether crosstalk between the senses relies on similar mechanisms. In two consecutive experiments, we used a task in which human participants (male and female) matched amplitude changes of concurrent visual, auditory and tactile stimuli. In this task, matching of congruent stimuli was associated with a behavioral benefit compared to matching of incongruent stimuli. In the first experiment, we used source-level analysis of high-density electroencephalography (EEG) and observed that cross-modal matching of congruent inputs was associated with relatively weaker coherence between gamma oscillations in early sensory regions. Next, we used bifocal high-definition transcranial alternating current stimulation (hd-tACS) to manipulate the strength of coupling between sensory cortices. Here, we used a lateralized version of the task in which hd-tACS was applied either ipsilateral or contralateral to the hemisphere receiving sensory stimuli. Ipsilateral gamma, but not alpha stimulation slowed responses to congruent trials whereas responding to incongruent trials was not changed by tACS. We speculate that fast responding to congruent stimuli involves decoupling of sensory gamma oscillations, which was prevented by tACS. These results indicate that synchronization of gamma oscillations promotes direct communication between sensory modalities. The framework of coupled gamma oscillations underlying cortical communication might thus be generalizable from processing within sensory streams to interactions between sensory networks.

Significance statement

Cortical gamma oscillations structure segregated neural activity and were suggested to represent a fundamental mechanism of network communication. While there is ample evidence for the role of long-range gamma synchronization in unisensory processing, its significance in multisensory networks is still unclear. We show that direct interactions between sensory cortices rely on synchronization of gamma band activity. To that end, we carried out two consecutive experiments using state-of-the-art high-density electroencephalography (EEG) and high-definition transcranial alternating current stimulation (hd-tACS). By complementing an observational with an interventional method, we provide novel evidence for the role of synchronized gamma oscillations in multisensory communication.

Introduction

Fast neuronal activity in the gamma range (>30 Hz) is a ubiquitous phenomenon in cortical networks and is thought to index local cortical computations (Fries, 2009; Donner and Siegel, 2011; Jia and Kohn, 2011). Both animal and human studies showed converging evidence that sensory processes, but also cognitive functions including attention and memory, are related to synchronization of gamma band activity (Gray et al., 1989; Engel et al., 2001; Herrmann et al., 2004; Siegel et al., 2008; Kerkoerle et al., 2014; Friese et al., 2016). Despite a broad agreement on the relevance of gamma oscillations, the elucidation of its mechanistic role is still ongoing. Early experiments provided supporting evidence for the claim that the synchronization of gamma oscillations corresponds to a relational code underlying perceptual grouping and feature integration (Gray et al., 1989; Engel et al., 1991; Neuenschwander et al., 1996; Gray, 1999). Taking a network perspective, synchronization of segregated neuronal groups was also suggested to enhance impact on downstream areas (Singer, 1999; Engel et al., 2001). Assuming ongoing gamma oscillations in these areas, it was proposed that effective communication should rely on synchrony between sending and receiving network nodes (Fries, 2005; Womelsdorf et al., 2007). Thus, for instance, attentional selection of visual inputs was shown to modulate gamma synchrony between V1 and V4 in the macaque (Bosman et al., 2012; Rohenkohl et al., 2018). Collectively, these results can be taken as evidence that the synchronization of gamma band activity organizes and enhances related sensory signals within modalities, and that synchronization along sensory streams routes information flow by gating windows for effective communication (Fries, 2009, 2015).

While there is good evidence for the validity of this proposal within sensory networks, it is unclear whether crosstalk between the senses relies on similar principles. A fundamental role of cross-modal interactions is the matching of stimulus features which allows to merge sensory inputs into a coherent multimodal representation of the environment where mutual information is amplified (Calvert et al., 1999). This amplification, often referred to as congruence enhancement, usually coincides with behavioral benefits (Schneider et al., 2008b; Göschl et al., 2014; Misselhorn et al., 2016). Senkowski et al. (2008) proposed that such cross-modal interactions might rely on synchronization of oscillatory rhythms. Here, we present two consecutive experiments designed to investigate the role of gamma oscillations in multisensory networks. In a re-analysis of electroencephalography (EEG) data (Misselhorn et al., 2018), we show that cross-modal matching of amplitude changes in concurrent visual, auditory and tactile stimuli is associated with changes in coupling between gamma oscillations in early sensory regions. Subsequently, we used bifocal high-definition transcranial alternating current

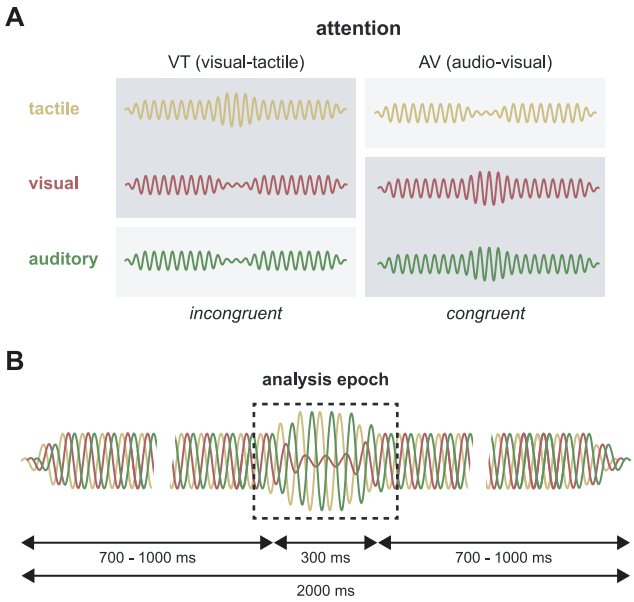

Figure 1. Experimental design of EEG experiment. (A) In different blocks, participants attended visual-tactile (VT) or audio-visual (AV) pairs out of a trimodal stimulus. Their task was to report whether the attended stimulus components changed congruently or incongruently. (B) Trimodal stimuli had a fixed duration of 2000 ms with a jittered onset of the amplitude change which lasted for 300 ms. Analyses were performed for the period of change.

stimulation (hd-tACS) to modulate sensory coupling. Importantly, both sensory and electrical stimulation were lateralized. We hypothesized that specific effects of tACS would occur only when electrical stimulation was administered ipsilateral to the hemisphere receiving sensory stimulation, but not when administered contralaterally. We show that ipsilateral stimulation with gamma, but not with alpha tACS modulated congruence-related benefits of cross-modal matching. Effects of contralateral tACS were unspecific with respect to the task, but were opposite with respect to stimulation frequency. We discuss alpha/gamma dynamics underlying cortical excitation as well as the putative role of long-range gamma synchronization in multisensory networks.

Methods

EEG experiment

Participants. Twenty-one participants (11 female, 23.8 ± 2.5 years) were invited for two sessions of EEG. None of them had a history of neurological or psychiatric disorders and visual, auditory and tactile perception were normal or corrected to normal. The experiment was approved by the ethics committee of the Hamburg Medical Association, all participants gave written consent and received monetary compensation for their participation.

Experimental design. Participants received trimodal sensory stimulation (see *Stimulus material* for details) on each trial of the experiment. These trimodal stimuli contained a visual, an auditory and a tactile component. On each trial, all components underwent a brief intensity change; that is, visual contrast, auditory loudness and vibration strength were either increased

or decreased. The task was to attend bimodal pairs (VT, visual-tactile or AV, audio-visual) blockwise and compare attended intensity changes (Figure 1 A). These changes could be either congruent (i.e., in the same direction) or incongruent (i.e., in different directions), the respective third modality had to be ignored. Blocks of VT and AV attention contained 64 trials with equal contributions of the eight possible stimulus configurations of increases and decreases across modalities. On two separate days, 10 blocks of each VT and AV attention were performed in an alternating fashion summing up to 1280 trials.

Stimulus material. Visual stimulation consisted of a circular, expanding grating presented centrally on a CRT screen (Iiyama, Model HM204DTA, refresh rate: 120 Hz) with grey background at a visual angle of 5°. The auditory stimulus component was a complex sinusoidal tone (13 sine waves: 64 Hz and its first 6 harmonics as well as 91 Hz and its first 5 harmonics, low-frequency modulator: 0.8 Hz) played back with audiometric insert earphones binaurally at 70 dB (E-A-RTONE 3A, 3M, USA). The tactile component was a high-frequency vibration delivered to the fingertips of both index fingers (250 Hz on C2 tactors, Engineering Acoustics Inc., USA). Visual contrast, auditory loudness and vibration amplitude were experimentally modulated. In total, trimodal stimuli had a fixed duration of 2 s and changes in intensity lasted for 300 ms (Figure 1 B). Transitions were smoothed with cosine tapers and onsets were jittered across trials between 700 and 1000 ms after stimulus onset. The magnitude of change per modality and change direction was estimated individually with a psychometric step-function prior to experimental blocks on each day (Watson and Pelli, 1983).

EEG recordings. High-density EEG was recorded from 128 channels using active Ag/AgCl electrodes referenced to the nose (EasyCap, Germany) via BRAINAMP MR amplifiers (Brain Products, Germany) and digitised after analog filtering (low cutoff: 10 s, high cutoff: 1000 Hz, sampling rate: 1000 Hz). After down-sampling to 500 Hz, data was filtered (high-pass: 1 Hz, low-pass: 120 Hz, notch: 49-51 Hz, 99-101 Hz) and cut into epochs locked to stimulus onset (-500 to 2000 ms). Prior to pre-processing, EEG was re-referenced to the common average. Dual-band independent components analysis (ICA) was used to remove stereotypical artifacts including eyeblinks, saccades, electrocardiogram and other myogenic activity (lower band: 1-30 Hz, higher band: 30-120 Hz). Due to low signal-to-noise ratio, 19 electrodes of the outer rim covering neck and chin were removed. Stratified data held on average 426 ± 89 epochs per participant. In sensor space, event-related potentials were averaged per experimental condition and subtracted from single-trial data. Source reconstruction was performed with exact low resolution electromagnetic tomography (eLORETA, regularisation: 0.05; Pascual-Marqui et al. 2011). Spatial filters were constructed using a three-shell head

model (Nolte and Dassios, 2005) and a cortical grid in MNI space obtained by down-sampling the Freesurfer template to 10000 grid points (Desikan et al., 2006). Dipole directions were constrained condition-wise and separately for the chosen frequencies of interest (see *Data analysis*) by maximizing spectral power of conditions with singular value decomposition.

Data analysis. Frequencies of interest in alpha/beta and gamma bands were defined by computing the global interaction measure (GIM) in sensor space (Ewald et al., 2012). GIM quantifies the overall strength of connectivity across all connections and yields a full spectrum, allowing to identify frequencies of maximal coupling. We computed GIM with a frequency resolution of 1 Hz based on whole trial data from all conditions (see Supplement 1). We defined peak frequencies for alpha/beta and gamma bands as the maximum between 8 and 20 Hz (alpha/beta) respectively 60 and 90 Hz (gamma). Individual peak frequencies for alpha/beta ranged from 9 to 16 Hz (13.19 $\pm$ 1.66 Hz) and for gamma from 60 to 90 Hz (77.19 $\pm$ 9.63 Hz). In source space, cross-spectra between all cortical grid points were computed at the frequencies of interest identified by GIM in a time window of 500 ms centred on the change. Imaginary coherence (iCoh) and power were computed by fast fourier transform using hanning windows (Nolte et al., 2004). Regions of interest (ROI) for primary visual, auditory and somatosensory cortex were defined anatomically by reference to the Freesurfer atlas (Desikan et al., 2006) and iCoh was averaged in bimodal networks for all edges between respective ROIs (i.e., visual-tactile, audio-visual and audio-tactile). In order to analyse systematic biases to the computation of iCoh, we estimated local synchronisation of cortical activity in the alpha/beta and gamma band. Event-related power was averaged for each ROI and subjected to analysis of variance (ANOVA) with factors *ROI* (visual/auditory/somatosensory), *ATTENTION* (VT/AV) and *CONGRUENCE* (congruent/incongruent) separately for alpha/beta and gamma bands. Similarly, iCoh was analysed by ANOVA with factors *NETWORK* (visual-tactile/audio-visual/audio-tactile), *ATTENTION* (VT/AV) and *CONGRUENCE* (congruent/incongruent) separately for alpha/beta and gamma bands. Where necessary, Greenhouse-Geisser correction was applied. Tables containing complete results from ANOVA can be found in Supplement 2.

tACS experiment

Participants. Twenty-four participants, who had not been enrolled in the EEG experiment, were recruited. All completed a training session after which four participants dropped out due to insufficient performance (<60 % accuracy). Twenty participants completed all experimental sessions (13 female, 25.3 ± 4.5 years). None of them had a history of neurological or psychiatric disorders and visual, auditory and tactile perception were normal or

corrected to normal. All gave written consent and received monetary compensation after completion of all three sessions. The Hamburg Medical Association approved the experiment.

Experimental design. The task of the tACS experiment was a simplified version of the task employed in the EEG experiment. Details of stimulus material outlined above apply here as well. Instead of trimodal stimuli, only visual-tactile stimulus pairs were presented in the right or left hemifield and to the right or left hand, respectively. Attention was cued by a centrally presented arrow prior to each trial and hemifields were chosen randomly but evenly throughout the experimental blocks. At all times, participants maintained fixation on a central fixation cross. Again, participants were asked to evaluate congruency of change directions. After a training session, participants completed two identical experimental sessions containing three blocks holding 192 trials. Experimental session used either alpha (10 Hz) or gamma (40 Hz) stimulation. These canonical stimulation frequencies were chosen because previous studies showed behavioural as well as neurophysiological effects for these frequencies (Helfrich et al., 2014a; Schwab et al., 2018). The order of experimental sessions was counterbalanced across participants. Experimental blocks featured in-phase, anti-phase or sham stimulation (see *Electrical stimulation* for details). The order of stimulation conditions was counter-balanced across participants.

Electrical stimulation. Alternating currents were administered in 4-in-1 montages with current flow between four outer and one central electrode (Patel et al., 2009; Saturnino et al., 2015) using Ag/AgCl ring electrodes (diameter = 12 mm). This configuration results in focal electric fields with peaks underneath the central electrode (Figure 3 A). For each participant, we prepared two of these montages designed to target primary visual and primary somatosensory cortex of one hemisphere, respectively. The side of stimulation was counterbalanced across participants. In conjunction with the lateralised experimental design, this resulted in equal proportions of trials that have electrical stimulation contra- or ipsilateral to the hemisphere receiving sensory stimulation. Prior to experimental blocks, stimulation was ramped up to 2mA peak-to-peak within 10 s. Sham blocks started with the same ramps, but included no stimulation thereafter. For in-phase stimulation, we used the same waveforms for both montages. For anti-phase stimulation, one waveform was shifted by 180°. In order to prevent inter-montage currents, two separate DC-stimulators were used (DC-Stimulator Plus, Neuroconn, Germany). Stimulators were operated in external mode allowing to control current output via voltage input. The voltage signal was computed in Matlab and produced by a NI-DAQ device run with Labview (NI USB 6343, National Instruments, USA). Impedances of each of the four outer electrodes relative to the central electrode were kept comparable within

montages (10-100 kΩ). This is crucial because identical impedances were assumed for the simulation of electric fields.

Simulation of electric fields. Electrode positions for the 4-in-1 montages were chosen such that electric fields were maximised in visual and somatosensory areas. For the simulations, we used the same standard cortical MNI model and leadfield matrix L that had been used for the source-level analysis of EEG data. We then calculated the electric field $\vec{E}$ at location $\vec{x}$ by linear superposition of evoked fields of all injected currents α_i at stimulation electrodes $i = \{1,2,\dots,10\}$ as

$$\vec{E}(\vec{x}) = \sum_i (\vec{L}(\vec{x})\alpha_i).$$

Within visual and somatosensory regions, peak values of 0.3 V/m were reached using currents with peak values of 1 mA. Spatial specificity was high as field strengths rapidly decreased when moving away from the central electrode. This ensured that electrical stimulation was confined to the targeted regions of one hemisphere only.

Data analysis. The effects of tACS were evaluated by analysing response times (RTs) by ANOVA with factors *HEMISPHERE* (ipsilateral/contralateral), *FREQUENCY* (alpha/gamma), *STIMULATION* (sham/in-phase/anti-phase) and *CONGRUENCE* (congruent/incongruent). Interactions were followed up by computing reduced ANOVA models. Where necessary, Greenhouse-Geisser correction was applied. Tables containing complete results from ANOVA can be found in Supplement 3.

Results

Local and long-range synchronization of sensory oscillations

We analyzed power in and coherence between alpha/beta and gamma oscillations in cortical sensory areas. Source reconstructions of scalp EEG were analyzed in an epoch containing the whole change period (Figure 1 B). In order to capture sensory processes with reasonable sensitivity, we selected large ROIs for visual, auditory and somatosensory cortex based on the anatomical Freesurfer parcellation (Desikan et al., 2006). First, we computed raw power for alpha/beta and gamma bands within these regions to exclude biases for the quantification of functional coupling by imaginary coherence. Results of ANOVA with factors *ATTENTION* (VT/AV) and *CONGRUENCE* (congruent/incongruent) showed that power in both alpha/beta and gamma bands was comparable across ROIs and experimental conditions (all $p > .05$; Figure 2 B). Second, we computed absolute imaginary coherence between all ROIs and subsequently

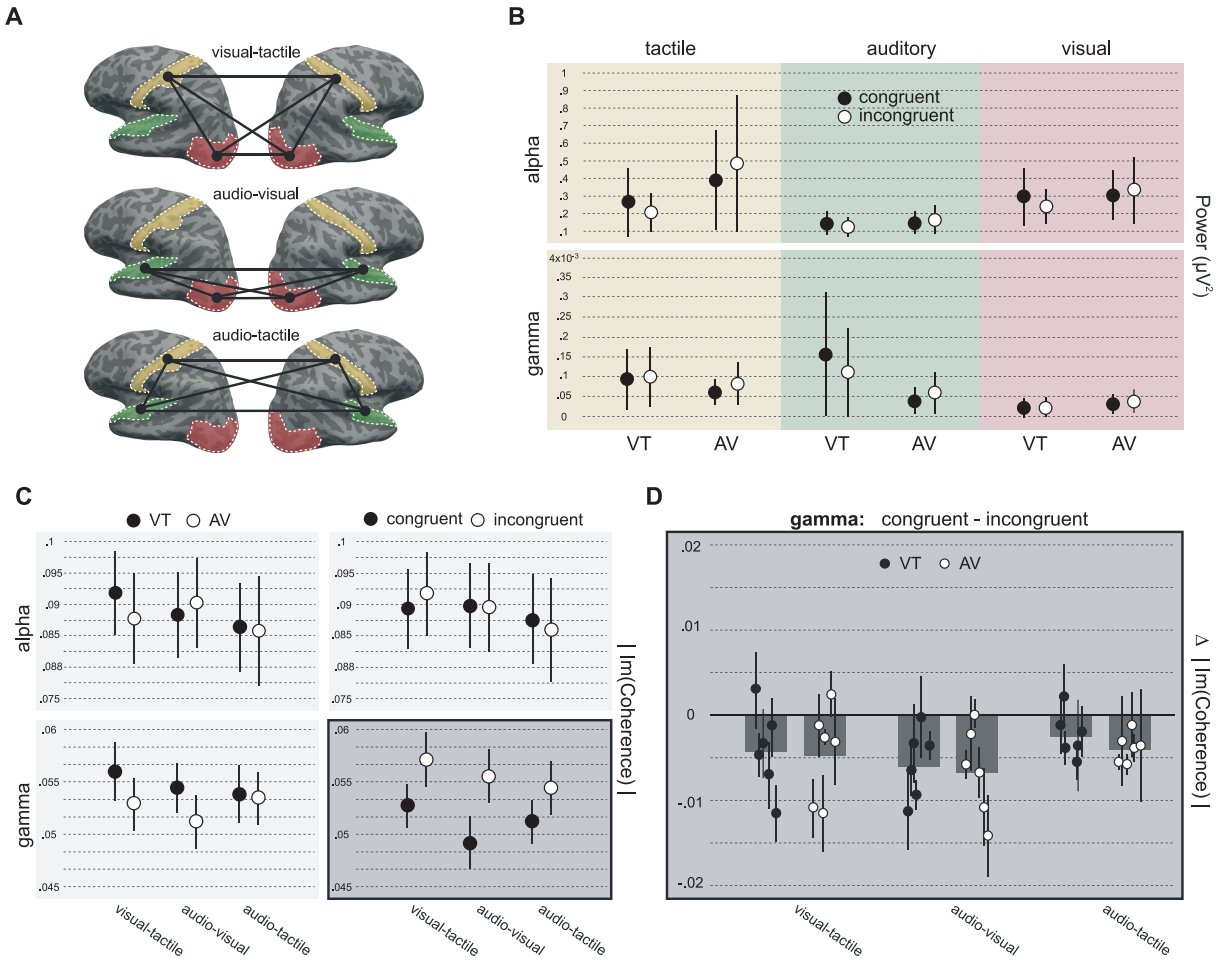

Figure 2. Results EEG experiment. (A) Schematic of analyzed network edges. Regions of interest (ROI) were based on the Freesurfer atlas (Red = visual cortex, green = auditory cortex, yellow = somatosensory cortex). (B) No effects of *ATTENTION* or *CONGRUENCE* on power in the alpha/beta and gamma bands for each ROI (same color coding as in (A)). Individual frequencies for the two bands were determined by global interaction measure (see *Methods* and Supplement 1). Black circles = congruent presentations, white circles = incongruent. (C) Absolute imaginary coherence, averaged over all edges of each network, shows a significant effect of *CONGRUENCE* in the gamma band only. (D) Effect of congruence displayed for individual edges of each network and attentional conditions.

averaged all edges of visual-tactile, audio-visual and audio-tactile networks (Figure 2 A). Based on the averaged networks, we computed an ANOVA on absolute imaginary coherence values. We found that gamma band coherence differed significantly by factor *CONGRUENCE* only ($F(1,20) = 6.666$, $p = 0.018$, $\eta_p^2 = 0.219$), revealing that synchronization in all networks was enhanced for incongruent relative to congruent trials (Figure 2 C,D). Although non-significant, larger absolute differences were observed for the task-relevant audio-visual and visual-tactile networks.

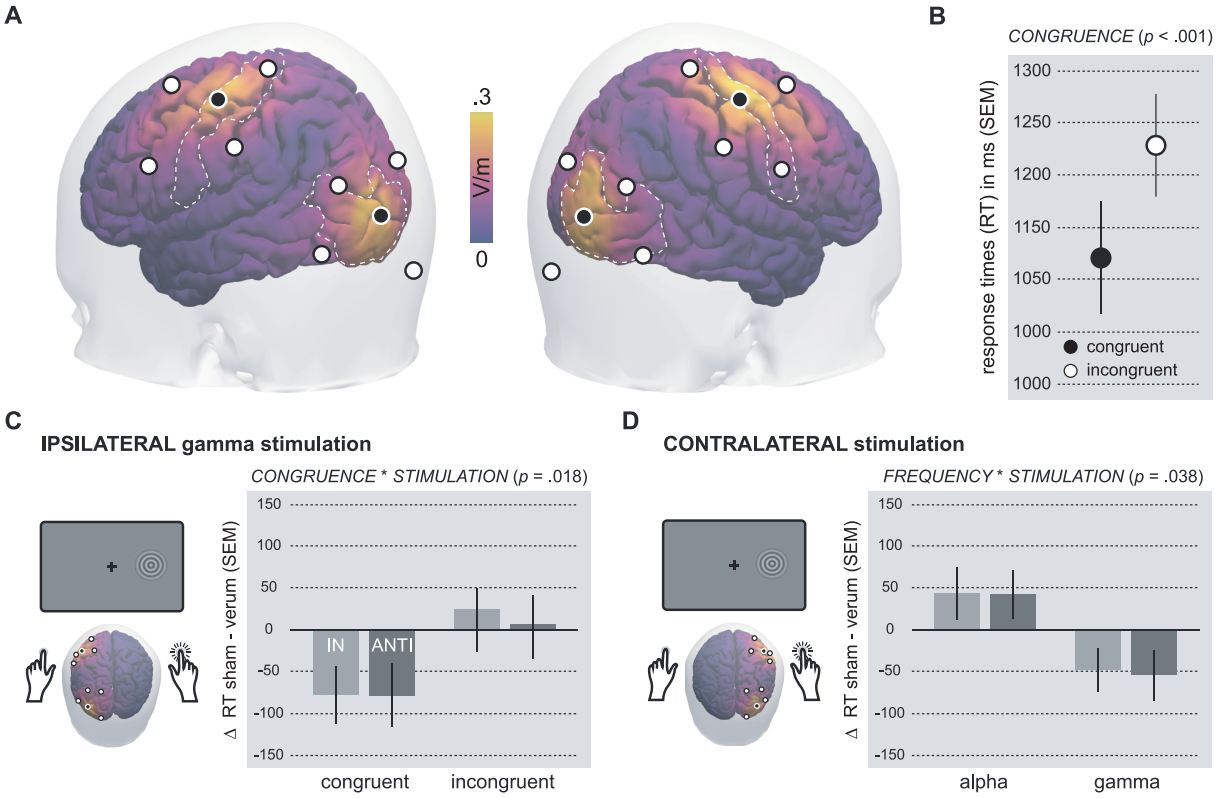

Figure 3. Results tACS experiment. (A) Electric fields distributions of bifocal hd-tACS over visual and somatosensory cortex. Alternating currents were applied with two separate left or right hemispheric 4-in-1 montages. Color coding on cortical surface corresponds to the simulated absolute field strength in V/m. (B) Behavioral effect of *CONGRUENCE* (error bars denote standard error of the mean). (C) *left:* The ipsilateral stimulation regime resulted in stimulation of the hemisphere receiving sensory input. *right:* Interaction between *CONGRUENCE* (congruent/incongruent) and *STIMULATION* (sham/in-phase/anti-phase) for ipsilateral gamma stimulation. Bars represent mean RT differences from sham for congruent and incongruent trials (error bars denote standard error of the mean). Separate bars for in- and anti-phase conditions show that phase did not influence behavior. (D) *left:* The contralateral stimulation regime resulted in stimulation of the hemisphere that did not receive sensory input. *right:* Interaction between *FREQUENCY* (alpha/gamma) and *STIMULATION* (sham/in-phase/anti-phase) for contralateral stimulation. Bars represent mean RT differences from sham for alpha and gamma stimulation (error bars denote standard error of the mean). Separate bars for in- and anti-phase conditions show that phase did not influence behavior.

Modulation of behavior with bifocal hd-tACS

In order to modulate coupling of sensory rhythmic activity, we applied in- or anti-phase tACS between visual and somatosensory cortex (0°/180° phase shift; Figure 3 A). Effects of gamma stimulation were controlled in three ways: (1) by using alpha as a control frequency, (2) by sham control, and (3) by stimulating in one hemisphere only (counter-balanced across participants) while visual-tactile stimuli were presented lateralized. Thus, hd-tACS could be either ipsilateral or contralateral with respect to the hemisphere receiving sensory stimuli (Figure 3 C,D). We hypothesized that only ipsilateral stimulation would affect cross-modal

matching performance. Specifically, we expected reductions in behavioral benefits of cross-modal congruence for ipsilateral gamma in-phase stimulation.

The behavioral effects of stimulation were analyzed with ANOVA comprising factors *HEMISPHERE* (ipsilateral/contralateral), *FREQUENCY* (alpha/gamma), *STIMULATION* (sham/in-phase/anti-phase) and *CONGRUENCE* (congruent/incongruent). Participants were well trained on the task and gave, on average, correct responses in ~83 % of all trials. Accuracy differed significantly between congruent and incongruent trials ($F(1,19) = 10.122$, $p = 0.005$, $\eta_p^2 = 0.348$), errors occurred less likely in congruent trials (85.48 %) when compared with incongruent trials (80.36 %). Timing of responses showed a similar, but stronger effect of *CONGRUENCE* ($F(1,19) = 34.659$, $p < 0.001$, $\eta_p^2 = 0.646$). Responses in congruent trials were on average faster than in incongruent trials (mean RT difference: 105 ms). Critically, the amount of behavioral benefit depended on all other factors (4-way interaction: $F(1.90,36.12) = 4.862$, $p = 0.015$, $\eta_p^2 = 0.204$). For ipsilateral gamma stimulation, we found a significant interaction between *CONGRUENCE* and *STIMULATION* ($F(1.93,36.65) = 4.578$, $p = 0.018$, $\eta_p^2 = 0.194$) (Figure 3 C). Although none of the post-hoc comparisons showed significant differences after correction for multiple comparisons, the interaction was driven by marked differences between sham and both stimulation conditions for incongruent trials (overall mean RT difference: 73 ms). For congruent trials, sham and stimulation conditions did not show notable differences (mean RT difference: 6 ms). Importantly, in- and anti-phase stimulation did not show significant differences (mean RT difference *congruent*: 2 ms; mean RT difference *incongruent*: 17 ms). Taken together, congruent trials under ipsilateral in- and anti-phase gamma stimulation showed impairments with respect to sham which were not seen for incongruent trials (Figure 3 C). Importantly, this interaction was absent for alpha stimulation ($F(1.80,34.23) = 2.079$, $p = 0.145$). Additionally, we found significant effects of contralateral stimulation, where responding was significantly influenced by the interaction between *FREQUENCY* and *STIMULATION* ($F(1.78,33.83) = 3.771$, $p = 0.038$, $\eta_p^2 = 0.166$) (Figure 3 D). Post-hoc comparisons showed positive, but non-significant differences between stimulation and sham for alpha frequency (mean RT difference: 48 ms) and negative, but non-significant differences for gamma frequency (mean RT difference: -50 ms). Thus, contralateral alpha stimulation showed improvements in overall performance while contralateral gamma stimulation showed impairments in overall performance when compared to sham.

Discussion

We investigated the putative role of long-range gamma synchronization between sensory cortices in multisensory perception. Importantly, spectral power in these regions was not modulated by the task. Instead, a previous whole-brain analysis of this EEG data showed that the power of alpha oscillations in frontal and parietal cortex was modulated by cross-modal attention (Misselhorn et al., 2018). In the current results, we observed coherence between sensory gamma oscillations to be associated with cross-modal congruence. Furthermore, we tested the relevance of this sensory coupling by intervention with non-invasive brain stimulation. As hypothesized, behavioral benefits of cross-modal congruence were modulated by bifocal gamma hd-tACS when administered ipsilaterally to the hemisphere receiving sensory stimulation. Contralateral stimulation produced global changes in performance that showed opposite effects for alpha and gamma stimulation.

Gamma coherence promotes communication between modalities

In our study, cross-modal matching between congruent inputs showed speeded responses when compared to the matching of incongruent inputs. This behavioral benefit of cross-modal congruence is well in line with previous studies that consistently showed faster responses, elevated accuracy, and better detection of congruent multisensory stimuli (e.g. Bolognini et al., 2004; Schneider et al., 2008b; Göschl et al., 2014; Misselhorn et al., 2016). While some studies demonstrated that these behavioral benefits likely relate to modulations of gamma power in temporal cortex (Schneider et al., 2008a, 2011), others showed that cross-modal interactions could also imply gamma power changes in primary sensory regions (Kaiser et al., 2006; Krebber et al., 2015). Besides local synchronization of gamma activity, there is evidence for inter-areal coupling of gamma oscillations supporting cross-modal processing (Keil and Senkowski, 2018). For instance, some studies showed that increased integration between sensory modalities was related to enhanced gamma band connectivity between auditory and temporal cortex (Ghazanfar et al., 2008; Maier et al., 2008). Less clear, however, are direct interactions between early sensory cortices of different modalities. Here, we report that matching of congruent stimuli was related to a relative decrease in gamma band coherence between sensory cortices. Importantly, synchronizing sensory gamma oscillations by ipsilateral hd-tACS slowed responses to congruent trials while responses to incongruent trials were unchanged by tACS. We suggest that gamma band coherence between sensory cortices promotes multisensory communication. Behavioral benefits of cross-modal congruence would thus emerge by faster completion of the matching process. Based on the above cited literature,

it is possible that further processing of stimuli in regions of multisensory convergence as the temporal lobe would require sensory cortices to decouple. This was presumably prevented by applying hd-tACS, which may have kept channels for communication open (Fries, 2005). Collectively, our data provide evidence that gamma oscillations promote direct communication between sensory modalities, and that flexible coupling and decoupling of these oscillations might underlie efficient cross-modal matching.

Surprisingly, the phase relation between the two applied tACS fields (0° or 180° phase shift) did not show distinct effects. For both ipsilateral as well as contralateral stimulation, phase did not influence behavior. One explanation would be that the exact phase of induced electric fields is difficult to control, especially for higher frequencies. This is suggested by a study that found phase of electric currents and the resulting fields of multi-electrode tACS to exhibit a non-linear relationship (Alekseichuk et al., 2018). It must be noted, however, that the authors of that study did not use high-definition montages. On the other hand, there is behavioral evidence that the phase of bifocal stimulation can be meaningful (Polanía et al., 2012; Helfrich et al., 2014b; Miyaguchi et al., 2019). Moreover, a recent study showed that interhemispheric alpha coupling as measured by EEG can be manipulated with in- or anti-phasic hd-tACS (Schwab et al., 2018). Alternatively, it is possible that – unlike communication within sensory modalities – multisensory communication is rather broadly tuned in frequency. In our EEG data, gamma frequencies of maximal coupling varied between 60 and 90 Hz without showing a clear peak on the group level (mean peak frequency: 77.19 Hz, see also Supplement 1). This is consistent with the literature where gamma band peak frequency usually shows large inter-individual variability (e.g. Schwarzkopf et al., 2012). Moreover, bandwidth of sensory gamma oscillations varies between modalities in a range between 30 and more than 100 Hz (*visual:* Jia et al. 2011; Friese et al. 2016; Sumner et al. 2018; *somatosensory:* Wahnoun et al. 2015; Ryun et al. 2017; von Lautz et al. 2017; *auditory:* Edwards et al. 2005; Griffiths et al. 2010; Mulert et al. 2011). Given this large variability within and across modalities, narrow tuning of direct multisensory communication channels would be surprising. It is thus possible that cross-modal interactions are rather broadly tuned, and that 40 Hz tACS in this study produced rather broad-band than frequency-specific effects.

Lateralized alpha/gamma activity regulates cortical excitability

Alpha and gamma oscillations have been proposed to implement functionally opposing mechanisms in cortex: while gamma oscillations are enhanced from activated cortical areas (Donner and Siegel, 2011), alpha oscillations predominate in task-irrelevant cortical regions

(Jensen and Mazaheri, 2010). This view is supported by a negative respectively positive correlation of EEG gamma and alpha power with the BOLD signal (Goldman et al., 2002; Ojemann et al., 2013). Importantly, the level of ongoing alpha activity could be shown to be a readout of cortical excitability as determined by transcranial magnetic stimulation (Romei et al. 2008). Cortical excitability, as controlled by alpha/gamma dynamics, is also discussed as a mechanism underlying top-down control of perceptual processes (Jensen and Mazaheri, 2010; Bonnefond and Jensen, 2015). For instance, cued spatial attention led to a lateralization of pre-stimulus alpha power to the task-irrelevant hemisphere, while stimulus-related gamma activity was lateralized to the task-relevant hemisphere (Marshall et al., 2015). In our tACS experiment, stimuli were presented lateralized and pre-trial cues were used to guide spatial attention of participants. Interestingly, alpha and gamma stimulation showed global, but opposite effects on response timing when administered over the task-irrelevant hemisphere: while alpha stimulation shortened response times, gamma stimulation led to delayed responses. We propose that reducing cortical excitability of the task-irrelevant hemisphere through alpha stimulation improved processing in the task-relevant hemisphere. Conversely, gamma stimulation might have increased excitability of the task-irrelevant hemisphere and thereby disrupted processing in the task-relevant hemisphere. A similar result has recently been obtained for unilateral stimulation over temporo-parietal cortex in a dichotic listening task (Wöstmann et al., 2018). In their study, alpha stimulation decreased recall of contralateral items while gamma stimulation showed the opposite effect. Our results, thus, add to the abundant literature that suggests an important role of alpha/gamma dynamics in modulating cortical excitability.

Limitations and future directions

Despite the complementary nature of the two presented experiments, investigating two distinct groups of participants was a limiting factor. Thus, we were not able to tailor the tACS stimulation frequencies individually based on preceding EEG recordings. However, using canonical stimulation frequencies, our data shows that such tailoring might not be necessary because tACS might influence relevant frequency bands rather broadly instead of narrow-banded. Future studies addressing the spectral profile of tACS-related changes in cortical activity will be helpful. Furthermore, analyses aimed at finding correlations between tACS-modulated behavior and electrophysiology were not possible. Ideally, such relations should be established within the same dataset. This is currently hampered by the unsolved problem of correcting tACS-related artifacts in electrophysiological recordings (Noury et al., 2016).

Meanwhile, future studies could resort to intermittent stimulation protocols that make use of potentially occurring aftereffects.

Conclusions

Our results from consecutive EEG and tACS experiments provide consistent evidence for an important role of coordinated gamma oscillations in early sensory regions for direct cross-modal communication. We thus suggest that effective cortical communication and information transfer between modalities involves similar principles as demonstrated for processing within sensory streams, namely the selective inter-areal synchronization of gamma oscillations. The pattern of results suggests that efficient matching between modalities may involve flexible coupling and decoupling of sensory gamma oscillations. Finally, we provide evidence for the idea that lateralized alpha/gamma dynamics are related to fluctuations of cortical excitability underlying selective attention.

References

Alekseichuk I, Falchier AY, Linn G, Xu T, Milham MP, Schroeder CE, Opitz A (2018) Electric field dynamics in the brain during multi-electrode transcranial electric stimulation. bioRxiv:340224.

Bolognini N, Frassinetti F, Serino A, Làdavas E (2004) "Acoustical vision" of below threshold stimuli: interaction among spatially converging audiovisual inputs. Exp Brain Res 160:273–282.

Bonnefond M, Jensen O (2015) Gamma Activity Coupled to Alpha Phase as a Mechanism for Top-Down Controlled Gating. PLoS ONE 10:e0128667.

Bosman CA, Schoffelen J-M, Brunet N, Oostenveld R, Bastos AM, Womelsdorf T, Rubehn B, Stieglitz T, De Weerd P, Fries P (2012) Attentional Stimulus Selection through Selective Synchronization between Monkey Visual Areas. Neuron 75:875–888.

Calvert GA, Brammer MJ, Bullmore ET, Campbell R, Iversen SD, David AS (1999) Response amplification in sensory-specific cortices during crossmodal binding. Neuroreport 10:2619–2623.

Desikan RS, Ségonne F, Fischl B, Quinn BT, Dickerson BC, Blacker D, Buckner RL, Dale AM, Maguire RP, Hyman BT, Albert MS, Killiany RJ (2006) An automated labeling system for subdividing the human cerebral cortex on MRI scans into gyral based regions of interest. NeuroImage 31:968–980.

Donner TH, Siegel M (2011) A framework for local cortical oscillation patterns. Trends Cogn Sci 15:191–199.

Edwards E, Soltani M, Deouell LY, Berger MS, Knight RT (2005) High gamma activity in response to deviant auditory stimuli recorded directly from human cortex. J Neurophysiol 94:4269–4280.

Engel AK, Fries P, Singer W (2001) Dynamic predictions: oscillations and synchrony in top-down processing. Nat Rev Neurosci 2:704–716.

Engel AK, Konig P, Kreiter AK, Singer W (1991) Interhemispheric synchronization of oscillatory neuronal responses in cat visual cortex. Science 252:1177–1179.

Ewald A, Marzetti L, Zappasodi F, Meinecke FC, Nolte G (2012) Estimating true brain connectivity from EEG/MEG data invariant to linear and static transformations in sensor space. NeuroImage 60:476–488.

Fries P (2005) A mechanism for cognitive dynamics: neuronal communication through neuronal coherence. Trends Cogn Sci 9:474–480.

Fries P (2009) Neuronal gamma-band synchronization as a fundamental process in cortical computation. Annu Rev Neurosci 32:209–224.

Fries P (2015) Rhythms for Cognition: Communication through Coherence. Neuron 88:220–235.

Friese U, Daume J, Göschl F, König P, Wang P, Engel AK (2016) Oscillatory brain activity during multisensory attention reflects activation, disinhibition, and cognitive control. Sci Rep 6:32775.

Ghazanfar AA, Chandrasekaran C, Logothetis NK (2008) Interactions between the superior temporal sulcus and auditory cortex mediate dynamic face/voice integration in rhesus monkeys. J Neurosci 28:4457–4469.

Goldman RI, Stern JM, Engel J, Cohen MS (2002) Simultaneous EEG and fMRI of the alpha

rhythm. Neuroreport 13:2487–2492.

Göschl F, Engel AK, Friese U (2014) Attention modulates visual-tactile interaction in spatial pattern matching. PloS One 9:e106896.

Gray CM (1999) The temporal correlation hypothesis of visual feature integration: still alive and well. Neuron 24:31–47, 111–125.

Gray CM, König P, Engel AK, Singer W (1989) Oscillatory responses in cat visual cortex exhibit inter-columnar synchronization which reflects global stimulus properties. Nature 338:334–337.

Griffiths TD, Kumar S, Sedley W, Nourski KV, Kawasaki H, Oya H, Patterson RD, Brugge JF, Howard MA (2010) Direct recordings of pitch responses from human auditory cortex. Curr Biol 20:1128–1132.

Helfrich RF, Knepper H, Nolte G, Strüber D, Rach S, Herrmann CS, Schneider TR, Engel AK (2014a) Selective Modulation of Interhemispheric Functional Connectivity by HD-tACS Shapes Perception. PLoS Biol 12:e1002031.

Helfrich RF, Schneider TR, Rach S, Trautmann-Lengsfeld SA, Engel AK, Herrmann CS (2014b) Entrainment of Brain Oscillations by Transcranial Alternating Current Stimulation. Curr Biol 24:333–339.

Herrmann CS, Munk MHJ, Engel AK (2004) Cognitive functions of gamma-band activity: memory match and utilization. Trends Cogn Sci 8:347–355.

Jensen O, Mazaheri A (2010) Shaping Functional Architecture by Oscillatory Alpha Activity: Gating by Inhibition. Front Hum Neurosci 4:186.

Jia X, Kohn A (2011) Gamma Rhythms in the Brain. PLOS Biol 9:e1001045.

Jia X, Smith MA, Kohn A (2011) Stimulus selectivity and spatial coherence of gamma components of the local field potential. J Neurosci 31:9390–9403.

Kaiser J, Hertrich I, Ackermann H, Lutzenberger W (2006) Gamma-band activity over early sensory areas predicts detection of changes in audiovisual speech stimuli. NeuroImage 30:1376–1382.

Keil J, Senkowski D (2018) Neural Oscillations Orchestrate Multisensory Processing. The Neuroscientist 24:609–626.

Kerkoerle T van, Self MW, Dagnino B, Gariel-Mathis M-A, Poort J, Togt C van der, Roelfsema PR (2014) Alpha and gamma oscillations characterize feedback and feedforward processing in monkey visual cortex. Proc Natl Acad Sci 111:14332–14341.

Krebber M, Harwood J, Spitzer B, Keil J, Senkowski D (2015) Visuotactile motion congruence enhances gamma-band activity in visual and somatosensory cortices. NeuroImage 117:160–169.

Maier JX, Chandrasekaran C, Ghazanfar AA (2008) Integration of bimodal looming signals through neuronal coherence in the temporal lobe. Curr Biol 18:963–968.

Marshall TR, O'Shea J, Jensen O, Bergmann TO (2015) Frontal eye fields control attentional modulation of alpha and gamma oscillations in contralateral occipitoparietal cortex. J Neurosci 35:1638–1647.

Misselhorn J, Daume J, Engel AK, Friese U (2016) A matter of attention: Crossmodal congruence enhances and impairs performance in a novel trimodal matching paradigm. Neuropsychologia 88:113–122.

Misselhorn J, Friese U, Engel AK (2018) Frontal and parietal alpha oscillations reflect attentional modulation of cross-modal matching. bioRxiv:477034.

Miyaguchi S, Otsuru N, Kojima S, Yokota H, Saito K, Inukai Y, Onishi H (2019) Gamma tACS over M1 and cerebellar hemisphere improves motor performance in a phase-specific manner. Neurosci Lett 694:64–68.

Mulert C, Kirsch V, Pascual-Marqui R, McCarley RW, Spencer KM (2011) Long-range synchrony of γ oscillations and auditory hallucination symptoms in schizophrenia. Int J Psychophysiol 9:55–63.

Neuenschwander S, Engel AK, König P, Singer W, Varela FJ (1996) Synchronization of neuronal responses in the optic tectum of awake pigeons. Vis Neurosci 13:575–584.

Nolte G, Bai O, Wheaton L, Mari Z, Vorbach S, Hallett M (2004) Identifying true brain interaction from EEG data using the imaginary part of coherency. Clin Neurophysiol Off J Int Fed Clin Neurophysiol 115:2292–2307.

Nolte G, Dassios G (2005) Analytic expansion of the EEG lead field for realistic volume conductors. Phys Med Biol 50:3807–3823.

Noury N, Hipp JF, Siegel M (2016) Physiological processes non-linearly affect electrophysiological recordings during transcranial electric stimulation. NeuroImage 140:99–109.

Ojemann GA, Ramsey NF, Ojemann J (2013) Relation between functional magnetic resonance imaging (fMRI) and single neuron, local field potential (LFP) and electrocorticography (ECoG) activity in human cortex. Front Hum Neurosci 7:34.

Pascual-Marqui RD, Lehmann D, Koukkou M, Kochi K, Anderer P, Saletu B, Tanaka H, Hirata K, John ER, Prichep L, Biscay-Lirio R, Kinoshita T (2011) Assessing interactions in the brain with exact low-resolution electromagnetic tomography. Philos Transact A Math Phys Eng Sci 369:3768–3784.

Patel J, Bansal V, Minha P, Ho J, Datta A, Bikson M (2009) High-Density Transcranial Direct Current Stimulation (HD-tDCS): Skin Safety and Comfort. J Med Devices 3:027554-027554–1.

Polanía R, Nitsche MA, Korman C, Batsikadze G, Paulus W (2012) The Importance of Timing in Segregated Theta Phase-Coupling for Cognitive Performance. Curr Biol 22:1314–1318.

Rohenkohl G, Bosman CA, Fries P (2018) Gamma Synchronization between V1 and V4 Improves Behavioral Performance. Neuron 100:953-963.e3.

Romei V, Brodbeck V, Michel C, Amedi A, Pascual-Leone A, Thut G (2008) Spontaneous Fluctuations in Posterior α-Band EEG Activity Reflect Variability in Excitability of Human Visual Areas. Cereb Cortex 18:2010–2018.

Ryun S, Kim JS, Lee H, Chung CK (2017) Tactile Frequency-Specific High-Gamma Activities in Human Primary and Secondary Somatosensory Cortices. Sci Rep 7:15442.

Saturnino GB, Antunes A, Thielscher A (2015) On the importance of electrode parameters for shaping electric field patterns generated by tDCS. NeuroImage 120:25–35.

Schneider TR, Debener S, Oostenveld R, Engel AK (2008a) Enhanced EEG gamma-band activity reflects multisensory semantic matching in visual-to-auditory object priming. NeuroImage 42:1244–1254.

Schneider TR, Engel AK, Debener S (2008b) Multisensory Identification of Natural Objects in a Two-Way Crossmodal Priming Paradigm. Exp Psychol 55:121–132.

Schneider TR, Lorenz S, Senkowski D, Engel AK (2011) Gamma-Band Activity as a Signature for Cross-Modal Priming of Auditory Object Recognition by Active Haptic Exploration. J Neurosci 31:2502–2510.

Schwab BC, Misselhorn J, Engel AK (2018) Modulation of interhemispheric alpha-band connectivity by transcranial alternating current stimulation. bioRxiv:484014.

Schwarzkopf DS, Robertson DJ, Song C, Barnes GR, Rees G (2012) The frequency of visually induced gamma-band oscillations depends on the size of early human visual cortex. J Neurosci 32:1507–1512.

Senkowski D, Schneider TR, Foxe JJ, Engel AK (2008) Crossmodal binding through neural coherence: implications for multisensory processing. Trends Neurosci 31:401–409.

Siegel M, Donner TH, Oostenveld R, Fries P, Engel AK (2008) Neuronal synchronization along the dorsal visual pathway reflects the focus of spatial attention. Neuron 60:709–719.

Singer W (1999) Neuronal Synchrony: A Versatile Code for the Definition of Relations? Neuron 24:49–65.

Sumner RL, McMillan RL, Shaw AD, Singh KD, Sundram F, Muthukumaraswamy SD (2018) Peak visual gamma frequency is modified across the healthy menstrual cycle. Hum Brain Mapp 39:3187–3202.

von Lautz AH, Herding J, Ludwig S, Nierhaus T, Maess B, Villringer A, Blankenburg F (2017) Gamma and Beta Oscillations in Human MEG Encode the Contents of Vibrotactile Working Memory. Front Hum Neurosci 11:576.

Wahnoun R, Benson M, Helms-Tillery S, Adelson PD (2015) Delineation of somatosensory finger areas using vibrotactile stimulation, an ECoG study. Brain Behav 5:e00369.

Watson AB, Pelli DG (1983) QUEST: a Bayesian adaptive psychometric method. Percept Psychophys 33:113–120.

Womelsdorf T, Schoffelen J-M, Oostenveld R, Singer W, Desimone R, Engel AK, Fries P (2007) Modulation of neuronal interactions through neuronal synchronization. Science 316:1609–1612.

Wöstmann M, Vosskuhl J, Obleser J, Herrmann CS (2018) Opposite effects of lateralised transcranial alpha versus gamma stimulation on auditory spatial attention. Brain Stimulat 11:752–758.

Supplement 1: Global interaction measure (GIM)

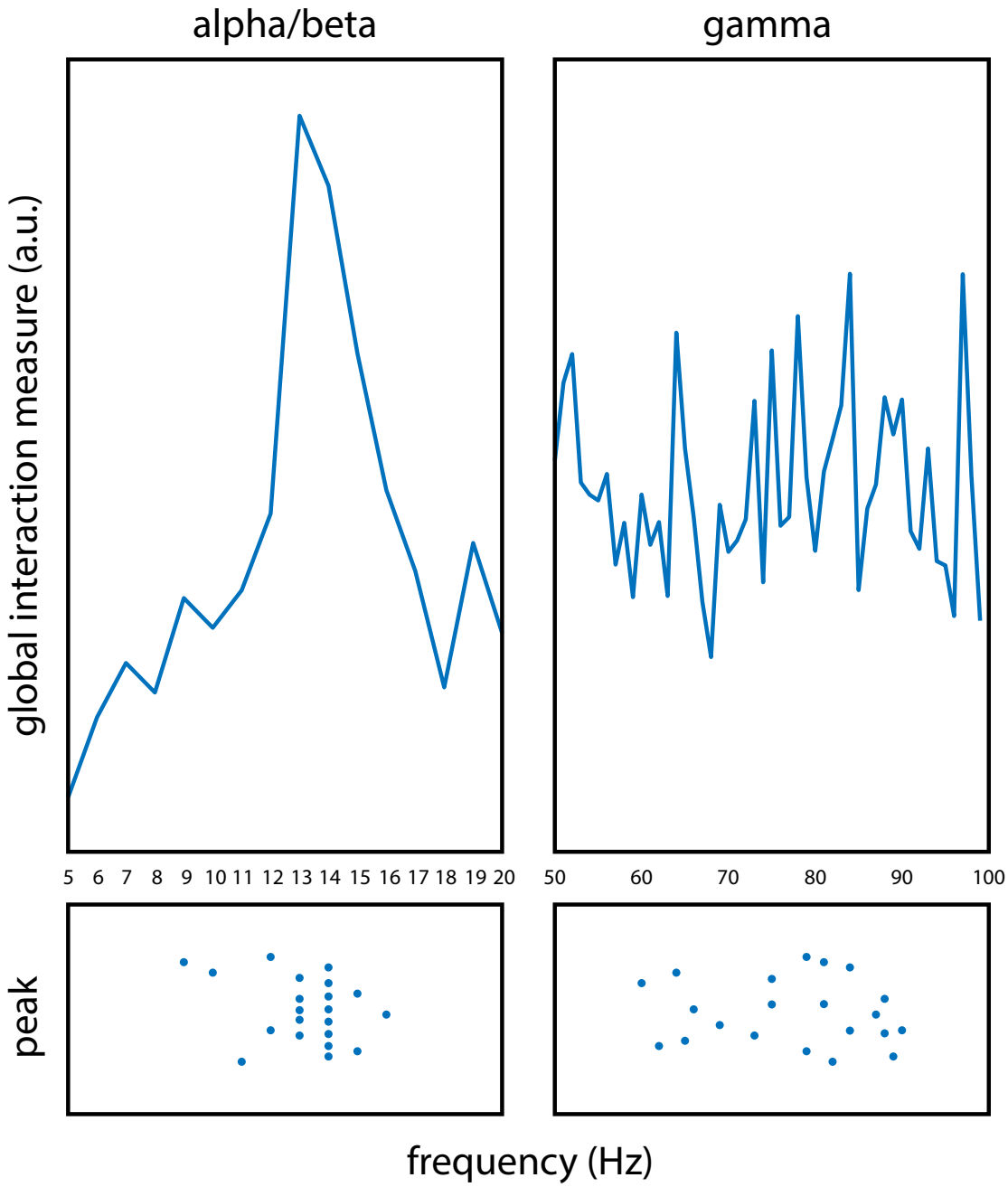

Spectra and individual peaks of GIM for sensory space EEG data. (top left) Spectrum from 5 to 20 Hz showing a clear group level peak at 13 Hz. (bottom left) Distribution of individual peak frequencies within a band from 8 to 20 Hz. (top right) Spectrum from 50 to 100 Hz does not show a distinct group level peak. (bottom right) Distribution of individual peak frequencies within a band from 60 to 90 Hz.

Supplement 2: Detailed statistics of EEG experiment

ANOVA alpha/beta power: network X attention X congruence

factor	**F**	p	η_p^2
network	1.096	0.313	0.052
attention	1.263	0.274	0.059
congruence	0.038	0.847	0.002
network*attention	1.106	0.306	0.052
network*congruence	1.411	0.255	0.066
attention*congruence	0.502	0.487	0.024
network*attention*congruence	0.769	0.390	0.038

ANOVA gamma power: network X attention X congruence

factor	**F**	p	η_p^2
network	0.904	0.353	0.043
attention	0.693	0.415	0.033
congruence	0.174	0.681	0.009
network*attention	0.958	0.339	0.046
network*congruence	0.840	0.375	0.040
attention*congruence	1.429	0.246	0.067
network*attention*congruence	1.420	0.247	0.066

ANOVA alpha/beta coherence: network X attention X congruence

factor	**F**	***p***	η_p^2
network	0.665	0.461	0.032
attention	0.085	0.774	0.004
congruence	0.522	0.478	0.025
network*attention	0.658	0.517	0.032
network*congruence	0.598	0.546	0.029
attention*congruence	0.088	0.770	0.004
network*attention*congruence	0.556	0.574	0.027

ANOVA gamma coherence: network X attention X congruence

factor	**F**	***p***	η_p^2
network	1.084	0.344	0.051
attention	0.784	0.386	0.038
congruence	5.623	0.028	0.219
network*attention	0.895	0.390	0.043
network*congruence	1.738	0.189	0.080
attention*congruence	0.023	0.882	0.001
network*attention*congruence	0.259	0.760	0.013

Supplement 3: Detailed statistics of tACS experiment

ANOVA ACC: hemisphere X frequency X stimulation X congruence

factor	**F**	***p***	η_p^2
hemisphere	0.741	0.400	0.038
frequency	0.652	0.429	0.033
stimulation	0.285	0.752	0.015
congruence	10.122	0.005	0.348
hemisphere*frequency	1.383	0.254	0.068
hemipshere*stimulation	1.589	0.223	0.077
frequency*stimulation	1.821	0.176	0.087
hemisphere*frequency*stimulation	2.783	0.074	0.128
hemisphere*congruence	1.833	0.192	0.088
frequency*congruence	2.621	0.122	0.121
hemisphere*frequency*congruence	0.130	0.723	0.007
stimulation*congruence	0.596	0.556	0.030
hemisphere*stimulation*congruence	1.494	0.239	0.073
frequency*stimulation*congruence	0.635	0.532	0.032
hemisphere*frequency*stimulation*congruence	0.587	0.559	0.030

ANOVA RT: hemisphere X frequency X stimulation X congruence

factor	**F**	***p***	η_p^2
hemisphere	0.355	0.558	0.018
frequency	0.02	0.888	0.001
stimulation	0.004	0.994	0.000
congruence	34.659	0.000	0.646
hemisphere*frequency	0.074	0.789	0.004
hemipshere*stimulation	0.057	0.934	0.003
frequency*stimulation	2.626	0.092	0.121
hemisphere*frequency*stimulation	1.543	0.229	0.075
hemisphere*congruence	0.140	0.713	0.007
frequency*congruence	0.013	0.910	0.001
hemisphere*frequency*congruence	0.004	0.949	0.000
stimulation*congruence	4.199	0.032	0.181
hemisphere*stimulation*congruence	0.256	0.728	0.013
frequency*stimulation*congruence	4.089	0.027	0.177
hemisphere*frequency*stimulation*congruence	4.862	0.015	0.204

ANOVA RT contralateral: frequency X stimulation X congruence

factor	**F**	***p***	η_p^2
frequency	0.030	0.864	0.002
stimulation	0.010	0.988	0.001
congruence	24.803	0.000	0.566
frequency*stimulation	3.771	0.038	0.166
frequency*congruence	0.015	0.904	0.001
stimulation*congruence	3.404	0.054	0.152
frequency*stimulation*congruence	0.163	0.841	0.008

ANOVA RT ipsilateral: frequency X stimulation X congruence

factor	**F**	***p***	η_p^2
frequency	0.012	0.913	0.001
stimulation	0.006	0.992	0.000
congruence	40.028	0.000	0.678
frequency*stimulation	1.459	0.246	0.071
frequency*congruence	0.001	0.971	0.000
stimulation*congruence	1.239	0.300	0.061
frequency*stimulation*congruence	7.548	0.002	0.284

ANOVA RT ipsilateral gamma tACS: stimulation X congruence

factor	**F**	***p***	η_p^2
stimulation	0.923	0.404	0.046
congruence	26.133	0.000	0.579
stimulation*congruence	4.578	0.018	0.194

ANOVA RT ipsilateral alpha tACS: stimulation X congruence

factor	**F**	***p***	η_p^2
stimulation	0.507	0.598	0.026
congruence	43.454	0.000	0.696
stimulation*congruence	2.079	0.145	0.099